Bull. Chem. Soc. Jpn. Vol. 82, No. 1, 86–92 (2009)

Hydrophobic Ionic Liquids Composed of Perfluoroalkyltrifluoroborates for Ionic Liquid–Water Two-Phase Systems

Naoya Nishi, Akihito Suzuki, and Takashi Kakiuchi*

Department of Energy and Hydrocarbon Chemistry, Graduate School of Engineering, Kyoto University, Kyoto 615-8510

Received August 14, 2008; E-mail: kakiuchi@scl.kyoto-u.ac.jp

Ionic liquids (ILs) composed of perfluoroalkyltrifluoroborate ions ($C_nF_{2n+1}BF_3^-$, $n = 2$, 3, 4, and 6) and highly hydrophobic cations are found to have properties suitable to the applications of ILs in IL–water (W) two-phase systems because of their high stability against hydrolysis, high hydrophobicity, and low melting points. The rate of hydrolysis of $C_nF_{2n+1}BF_3^-$ is four orders of magnitude slower than that of BF_4^-. The ion-transfer voltammograms for the transfer of $C_nF_{2n+1}BF_3^-$ across the interface between nitrobenzene and W show that these $C_nF_{2n+1}BF_3^-$ have hydrophobicity comparable to or higher than those of PF_6^- and bis(trifluoromethylsulfonyl)imide depending on n. The physicochemical properties (density, viscosity, conductivity, and solubility of ILs in W) of $C_nF_{2n+1}BF_3^-$-based ILs are measured for the ILs having melting points lower than room temperature. The hydrophobicity of the $C_nF_{2n+1}BF_3^-$ ions is well correlated with the solubility of the ILs in W and also with the width of the polarized potential window at the IL|W interface.

Two-phase systems composed of water (W) and hydrophobic ionic liquids (ILs) are promising for liquid–liquid extraction,[1–3] two-phase biotransformation,[4–6] and electrochemical devices such as ion-selective electrodes[7–9] and salt bridges.[10–12] The physicochemical properties of hydrophobic ILs can be tuned by choosing hydrophobic cations and anions constituting the ILs. A variety of hydrophobic cations such as imidazolium, pyridinium, quaternary ammonium, and quaternary phosphonium ions, are readily available. In contrast, the number of hydrophobic anions suitable to hydrophobic ILs with low melting points (T_m) is limited: for example, BF_4^-, PF_6^-, bis(trifluoromethylsulfonyl)imide ($C_1C_1N^-$), bis(pentafluoroethylsulfonyl)imide ($C_2C_2N^-$), $PF_3(C_2F_5)_3^-$, and $B(CN)_4^-$. It is known that BF_4^- [13–15] and PF_6^- [16–18] are hydrolyzed in the presence of water to produce HF. The produced HF can be a serious concern in application of IL–W two-phase systems.[3] For fine tuning of the properties of hydrophobic ILs used for IL–W two-phase systems, hydrophobic anions that are stable against hydrolysis and that form ILs having low T_m are highly desirable.

Imide ions such as $C_1C_1N^-$ and $C_2C_2N^-$ seem to be among the best choices for hydrophobic ILs. However, one problem of the imide ions is the complexation with metal ions in ILs[19–21] and at the IL|W interface.[22] The complexation in ILs or at the IL|W interface can lead to the shift of the phase-boundary potential across the IL|W interface. The shift is undesirable when IL–W two-phase systems are applied to electrochemical applications such as salt bridges and ion-selective electrodes. Anions that only weakly coordinate to metal ions are necessary for certain electrochemical applications of IL–W two-phase systems, especially for the salt bridges, which require anions having hydrophobicity similar to those of $C_1C_1N^-$ and $C_2C_2N^-$.[10]

It is known that BF_4^- is a weakly coordinating anion. The stability of BF_4^- against hydrolysis can be enhanced by substitution of F atoms in BF_4^- with perfluoroalkyl moieties.[23,24] In addition, this substitution increases the hydrophobicity of the anions, which is desirable for ions constituting hydrophobic ILs for IL–W two-phase systems. Frohn and Bardin reported a new method to synthesize perfluoroalkyltrifluoroborate ions, $C_nF_{2n+1}BF_3^-$ with $n = 3$ and 6.[25] Zhou et al. prepared ILs of $C_nF_{2n+1}BF_3^-$ ($n = 2$–4), and studied their physicochemical properties for electrochemical applications.[24,26–32]

In this study, by using $C_nF_{2n+1}BF_3^-$ ($n = 2$–4 and 6) in combination with highly hydrophobic cations, we prepared ILs that have high hydrophobicity, high stability against hydrolysis, and low melting point suitable for IL–W two-phase systems. We will show that the hydrophobicity of the $C_nF_{2n+1}BF_3^-$ ions is well correlated with the solubility of the ILs in W and also with the width of the polarized potential window at the IL|W interface.

Experimental

Synthesis of Anions. Potassium salts of $C_nF_{2n+1}BF_3^-$ ($n = 2$, 3, 4, and 6) were synthesized using a one-step method by Zhou et al.[33] that is a modification of a two-step method originally presented by Frohn and Bardin.[25] Phenylmagnesium bromide (Aldrich), trimethoxyborane (Wako Pure Chemical Industries), $C_nF_{2n+1}I$ (Daikin Industries for $n = 2$, Tokyo Chemical Industry for $n = 3$, 4, and 6), and hydrofluoric acid (46–48 wt %, Wako Pure Chemical Industries) were used for the synthesis. Potassium salts of $C_nF_{2n+1}BF_3^-$ were characterized by ^{19}F NMR and ^{11}B NMR.

^{19}F NMR. ^{19}F NMR spectra were recorded to evaluate the stability of $C_nF_{2n+1}BF_3^-$ in an aqueous solution using a 400 MHz NMR spectrometer (EX-400, JEOL). $K^+[C_nF_{2n+1}BF_3^-]$ was dissolved in D_2O at a concentration of 0.05 mol dm^{-3}. For acidic conditions, 1 mol dm^{-3} CF_3COOD was added to the solution. For experiments at a high temperature, the solution was kept in a water bath kept at 70 °C. CF_3COOD was used also as an internal standard; the chemical shift of the peak was assumed to be −76.5 ppm.

Published on the web January 14, 2009; doi:10.1246/bcsj.82.86

I	II	III	IV	V	
Ag/AgCl	10 mM $MgCl_2$	20 mM $[TPnA^+][TFPB^-]$	10 mM $MgCl_2$	AgCl/Ag	
	5 mM $[TPnA^+]Cl^-$	0.2wt% Span80	0.5 mM $K^+[C_nF_{2n+1}BF_3^-]$		(I)
	(W_{ref})	(NB)	(W)		

Scheme 1.

I	II	III	IV	V	
Ag/AgCl	20 mM LiCl	$[C^+][C_nF_{2n+1}BF_3^-]$	100 mM LiCl	AgCl/Ag	
	3 mM $[C^+]Cl^-$				(II)
	(W_{ref})	(IL)	(W in pipette)		

Scheme 2.

Preparation of ILs. Hydrophobic cations (C^+) used for the preparation of $C_nF_{2n+1}BF_3^-$-based ILs are 1-methyl-3-octylimidazolium (C_8mim^+), tetrabutylammonium (TBA^+), and tetrahexylammonium (THA^+) ions. $[C_8mim^+]Cl^-$ was synthesized from 1-methylimidazole (Aldrich) and 1-chlorooctane (Aldrich).[34] $[TBA^+]Cl^-$ and $[THA^+]Cl^-$ were purchased from Tokyo Chemical Industry and Aldrich, respectively. Equimolar amounts of $K^+[C_nF_{2n+1}BF_3^-]$ and $[C^+]Cl^-$ were dissolved in methanol. After evaporating methanol by a rotary evaporator, dichloromethane was added to the mixture of IL and KCl. The dichloromethane solution was repeatedly washed with Milli-Q water (Millipore) to remove KCl until no Cl^- ions were detected in the washing when an aqueous $AgNO_3$ solution was added. Dichloromethane as well as volatile impurities such as water and methanol were evaporated with an oil pump.

Measurements of Physicochemical Properties. A differential scanning calorimeter (Pyris Diamond DSC, Perkin-Elmer) was used to determine the melting point and the glass transition point for $C_nF_{2n+1}BF_3^-$-based ILs at a heating rate of 10 °C min^{-1}. A pycnometer, a viscometer (VM-10A-M, CBC Materials), and an ionic conductometer (CM-117, Kyoto Electronics Manufacturing) were used for measurements of the density, the viscosity, and the ionic conductivity for $C_nF_{2n+1}BF_3^-$-based ILs at 25.0 °C, respectively.

The solubility of $[C_8mim^+][C_nF_{2n+1}BF_3^-]$ ($n = 2$–4) in water was spectrophotometrically measured. The concentration of C_8mim^+ in W was measured with a molar absorption coefficient, 4.17×10^3 mol^{-1} dm^3 cm^{-1}, reported for $[C_8mim^+][BF_4^-]$ at 211 nm in W.[35] $[C_8mim^+][C_nF_{2n+1}BF_3^-]$ and water were mutually saturated by immersing the sample bottle containing them in a water bath at 25.0 ± 0.1 °C for more than 1 day.

Cyclic Voltammetry at the NB|W Interface. Cyclic voltammograms for the ion transfer across the NB|W interface were recorded with a four-electrode electrochemical cell at 25 °C. The details of the experimental setup have been described elsewhere.[36] The electrochemical cell is represented as shown in Scheme 1. M denotes mol dm^{-3}, $TPnA^+$ is tetrapentylammonium, and $TFPB^-$ is tetrakis[3,5-bis(trifluoromethyl)phenyl]borate. Platinum wires were used for the two counter electrodes in W and NB phases. The potential of phase **V** with respect to that of phase **I** is denoted as E. The potential was controlled with a four-electrode potentiostat (Potentiostat/Galvanostat, HA10100m1M1A, Hokuto Denko) with a positive feedback for the IR compensation. The current (I) due to the cation transfer from W to NB is taken to be positive. The area of the flat NB|W interface was 0.16 cm^2. Picrate ion (pic) was used for the reference anion to evaluate the apparent standard ion-transfer potentials ($\Delta_{NB}^{W}\phi_{i,app}^{0}$) of $C_nF_{2n+1}BF_3^-$. The adjective "apparent" means that the values are evaluated at finite concentrations of the supporting electrolytes in both NB and W. We assumed that the value of the diffusion-coefficient terms[37] in the mid-point potential, $E_{m,i}$, are the same for these anions and thus can be canceled out by subtraction:

$$\Delta_{NB}^{W}\phi_{i,app}^{0} - \Delta_{NB}^{W}\phi_{pic,app}^{0} = E_{m,i} - E_{m,pic} \qquad (1)$$

The value of $\Delta_{NB}^{W}\phi_{pic,app}^{0}$ in the literature, +0.069 V,[38] was used to evaluate $\Delta_{NB}^{W}\phi_{i,app}^{0}$ for $C_nF_{2n+1}BF_3^-$ from experimentally obtained $E_{m,i}$ and $E_{m,pic}$ using eq 1.

Cyclic Voltammetry at Ionic Liquid|Water Interface. Cyclic voltammograms at the IL|W interface formed at the tip of a micropipette were recorded at 25 °C for estimating the polarized potential window (ppw) of the IL|W interface.[39,40] The two-electrode electrochemical cell we employed is represented as shown in Scheme 2. The definition of E and I is the same as that for cyclic voltammetry at the NB|W interface.

Results and Discussion

Stability of $C_nF_{2n+1}BF_3^-$ Ions against Hydrolysis. BF_4^- is known to be hydrolyzed in water to produce $BF_{4-m}(OH)_m^-$.[14] We studied the stability of $C_nF_{2n+1}BF_3^-$ in aqueous solutions of $K^+[C_nF_{2n+1}BF_3^-]$ using ^{19}F NMR. Taking into account the fact that the rate of the hydrolysis of BF_4^- is accelerated at high temperature and low pH,[14] hydrolysis reactions in four conditions were compared, i.e., at room temperature (case **1**), at 70 °C (case **2**), at room temperature with 1 M CF_3COOD (case **3**), and at 70 °C with 1 M CF_3COOD (case **4**). In cases **1**–**3**, there was no discernible change in ^{19}F NMR spectra of $C_nF_{2n+1}BF_3^-$ after 300 h. However, in case **4** the ^{19}F NMR spectra varied with time. Figure 1 shows a region of ^{19}F NMR spectra for the CF_3 moiety of $C_2F_5BF_3^-$ after the solution was kept for 0, 40, 80, and 120 h in case **4**. After 40 h, small peaks appeared at two regions of −84.3 and −83.85 ppm, which were located at 0.5 and 0.95 ppm lower magnetic field region than the peak at −84.8 ppm assigned to the CF_3 moiety of $C_2F_5BF_3^-$. The height of the small peaks increased with time. Such small peaks at lower field also appeared in the spectrum regions of the CF_2 and BF_3^- moieties of $C_2F_5BF_3^-$ (data not

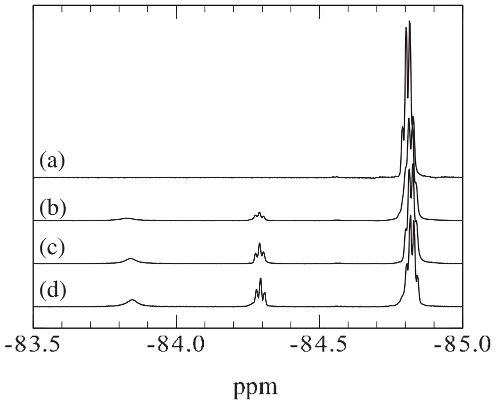

Figure 1. ^{19}F NMR spectra of 0.05 M $C_2F_5BF_3^-$ in deuterium oxide with 1 M CD_3COOD kept at 70 °C for (a) 0, (b) 40, (c) 80, and (d) 120 h.

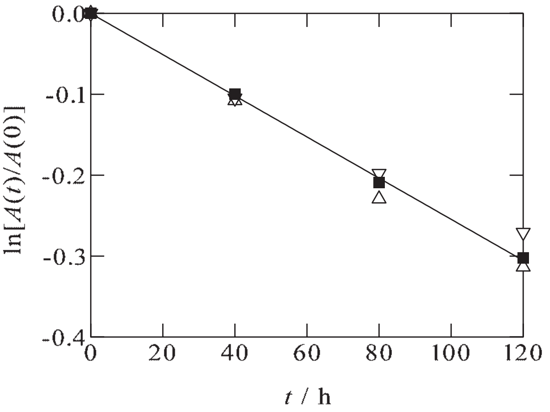

Figure 2. Time dependence of the normalized peak area of $C_2F_5BF_3^-$ for CF_3 (open triangle), CF_2 (solid square), and BF_3^- (open inverted triangle) moieties. The solid line is a linear regression line from the plots.

shown). The appearance of the small peaks at the lower magnetic field can be interpreted as weaker shielding of $C_2F_5BF_{3-m}(OH)_m^-$ than $C_2F_5BF_3^-$. This tendency was observed in a previous ^{19}F NMR study as lower magnetic field of peaks for $BF_{4-m}(OH)_m^-$ than those for BF_4^-.[41] A B3LYP/6-311+G** level calculation using Gaussian03[42] showed 0.4 and 1.1 ppm lower shielding constants for the CF_3 moiety of $C_2F_5BF_2OH^-$ and $C_2F_5BF(OH)_2^-$ than that of $C_2F_5BF_3^-$, respectively. The difference in the shielding constants in the calculation agrees with the observed difference in the experiment. The small peaks at −84.3 ppm can thus be assigned to $C_2F_5BF_2OH^-$ and the other at −83.85 ppm to $C_2F_5BF(OH)_2^-$. No peak that can be assigned to $C_2F_5B(OH)_3^-$ was found.

Since the hydrolysis of BF_4^- in acidic solutions is well known to be a first-order reaction where the rate is proportional to the concentration of BF_4^-,[43] we assumed that the rate of the hydrolysis of $C_2F_5BF_3^-$ is represented as $dc/dt = -kc$ where c is the concentration of $C_2F_5BF_3^-$ and k is the first-order rate constant. Figure 2 shows the time dependence of the natural logarithm of the peak area assigned to $C_2F_5BF_3^-$ normalized by that at $t = 0$, for CF_3, CF_2, and BF_3^- moieties of $C_2F_5BF_3^-$. The k value was evaluated to be 2.5×10^{-3} h^{-1} from the slope of a linear regression line from the plots shown in Figure 2.

Table 1. Rate Constants for Hydrolysis of $C_nF_{2n+1}BF_3^-$ and BF_4^- in 1 M Acid Aqueous Solution at 70 °C

Anion	k/h^{-1}
$C_2F_5BF_3^-$	2.5×10^{-3}
$C_3F_7BF_3^-$	1.5×10^{-3}
$C_4F_9BF_3^-$	1.5×10^{-3}
$C_6F_{13}BF_3^-$	1.1×10^{-3}
BF_4^-	8.5×10^{1} a)

a) Estimated from the equation for the temperature and pH dependence of the rate constant.[14]

Table 2. Apparent Standard Ion-Transfer Potentials of IL-Constituent Ions for the NB–W Two-Phase System

Ion	$\Delta_{NB}^{W}\phi_{i,app}^{0}$/V
BF_4^-	−0.124 a)
PF_6^-	0.025 a)
$C_2F_5BF_3^-$	0.06
$C_3F_7BF_3^-$	0.10
$C_1C_1N^-$	0.133 a)
$C_4F_9BF_3^-$	0.14
$C_6F_{13}BF_3^-$	0.22 b)
C_8mim^+	−0.235 a)
TBA^+	−0.281 a)
THA^+	−0.52 c)

a) Ref. 44. b) Extrapolated from the $\Delta_{NB}^{W}\phi_{i,app}^{0}$ values for $C_nF_{2n+1}BF_3^-$ ($n = 2$–4). c) Extrapolated from the $\Delta_{NB}^{W}\phi_{i,app}^{0}$ values[44] for symmetrical tetraalkylammonium ions (from methyl to pentyl).

Table 1 lists the rate constants for $C_nF_{2n+1}BF_3^-$ ($n = 2$, 4, and 6) in case **4**, and for BF_4^- under the same conditions estimated from the temperature and pH dependences of the rate constant in the literature.[14] The $C_nF_{2n+1}BF_3^-$ ions are found to have stability four orders of magnitude higher than BF_4^-. Among the $C_nF_{2n+1}BF_3^-$, ions with longer perfluoroalkyl chains are more stable but the difference is small compared with that between BF_4^- and $C_nF_{2n+1}BF_3^-$.

Hydrophobicity of $C_nF_{2n+1}BF_3^-$ Ions. $\Delta_{NB}^{W}\phi_{i,app}^{0}$ values as a hydrophobicity scale of $C_nF_{2n+1}BF_3^-$ ions were evaluated from ion-transfer cyclic voltammograms (CVs) across the NB|W interface. Table 2 shows the $\Delta_{NB}^{W}\phi_{i,app}^{0}$ values of $C_nF_{2n+1}BF_3^-$ along with those of the hydrophobic cations used in the present study and other common hydrophobic anions for ILs.[44] For anions, the more positive the value of $\Delta_{NB}^{W}\phi_{i,app}^{0}$ is, the more hydrophobic the ion is, and for cations vice versa. The $\Delta_{NB}^{W}\phi_{i,app}^{0}$ values of $C_nF_{2n+1}BF_3^-$ (0.06–0.22 V) are considerably more positive compared with that of BF_4^- (−0.124 V), indicating that the perfluoroalkyl moiety increases the hydrophobicity of the anions compared with BF_4^-. The hydrophobicity of $C_2F_5BF_3^-$ and that of $C_3F_7BF_3^-$ are between those of PF_6^- and $C_1C_1N^-$. The hydrophobicity of $C_4F_9BF_3^-$ is similar to that of $C_1C_1N^-$. $C_6F_{13}BF_3^-$ is the most hydrophobic among these IL-constituent anions. One can thus tune the hydrophobicity of an IL by choosing a RTIL-constituent anion from anions including $C_nF_{2n+1}BF_3^-$.

Melting Points, Density, Viscosity, and Conductivity for ILs of $C_nF_{2n+1}BF_3^-$. The T_m values of the ILs prepared from $C_nF_{2n+1}BF_3^-$ ($n = 2$, 3, 4, and 6) and several highly hydro-

Table 3. Physicochemical Properties (Melting Point (T_m), Density (d), Viscosity (η), Conductivity (κ), and Solubility of the ILs in Water ($S_{R/W}$)) for ILs of $C_nF_{2n+1}BF_3^-$ Prepared in the Present Study and of Other Hydrophobic Anions

IL	T_m/°C	d/g cm^{-3} a)	η/mPa s$^{a)}$	κ/mS cm^{-1} a)	$S_{R/W}$/mM$^{a)}$
$[C_8mim^+][BF_4^-]$	(−81$^{b)}$)$^{c)}$	1.103$^{d)}$	341$^{d)}$	0.58$^{e)}$	64$^{f)}$
$[C_8mim^+][C_2F_5BF_3^-]$	−6(−92$^{b)}$)	1.21	44.7	2.70	5.3
$[C_8mim^+][C_3F_7BF_3^-]$	10(−40$^{b)}$)	1.27	48.1	2.03	1.8
$[C_8mim^+][C_4F_9BF_3^-]$	9(−76$^{b)}$)	1.31	58.0	1.40	0.95
$[C_8mim^+][C_6F_{13}BF_3^-]$	37	—$^{g)}$	—$^{g)}$	—$^{g)}$	—$^{g)}$
$[C_8mim^+][PF_6^-]$	(−82$^{b)}$)$^{h)}$	1.22$^{h)}$	682$^{h)}$	0.25$^{e)}$	21$^{f)}$
$[C_8mim^+][C_1C_1N^-]$	−9.19$^{i)}$	1.320$^{j)}$	90.0$^{j)}$	1.3$^{j)}$	1.6$^{k)}$
$[TBA^+][BF_4^-]$	159–162$^{l)}$	—$^{g)}$	—$^{g)}$	—$^{g)}$	—$^{g)}$
$[TBA^+][C_2F_5BF_3^-]$	91	—$^{g)}$	—$^{g)}$	—$^{g)}$	—$^{g)}$
$[TBA^+][C_3F_7BF_3^-]$	65	—$^{g)}$	—$^{g)}$	—$^{g)}$	—$^{g)}$
$[TBA^+][C_4F_9BF_3^-]$	46	—$^{g)}$	—$^{g)}$	—$^{g)}$	—$^{g)}$
$[TBA^+][C_6F_{13}BF_3^-]$	15(−50$^{b)}$)	1.30	1440	0.0987	0.1$^{m)}$
$[TBA^+][PF_6^-]$	244–246$^{l)}$	—$^{g)}$	—$^{g)}$	—$^{g)}$	—$^{g)}$
$[TBA^+][C_1C_1N^-]$	91$^{n)}$	—$^{g)}$	—$^{g)}$	—$^{g)}$	—$^{g)}$
$[THA^+][BF_4^-]$	90–92$^{l)}$	—$^{g)}$	—$^{g)}$	—$^{g)}$	—$^{g)}$
$[THA^+][C_2F_5BF_3^-]$	19(−67$^{b)}$)	1.05	510	0.0417	0.04$^{m)}$
$[THA^+][C_3F_7BF_3^-]$	58	—$^{g)}$	—$^{g)}$	—$^{g)}$	—$^{g)}$
$[THA^+][C_4F_9BF_3^-]$	51	—$^{g)}$	—$^{g)}$	—$^{g)}$	—$^{g)}$
$[THA^+][C_6F_{13}BF_3^-]$	19(−58$^{b)}$)	1.19	997	0.0233	0.002$^{m)}$
$[THA^+][PF_6^-]$	135–138$^{l)}$	—$^{g)}$	—$^{g)}$	—$^{g)}$	—$^{g)}$
$[THA^+][C_1C_1N^-]$	−6.8$^{n)}$	1.11$^{n)}$	435$^{n)}$	0.11$^{n)}$	0.007$^{o)}$

a) At 25 °C. b) Glass transition point. c) Ref. 53. d) Ref. 54. e) Ref. 55. f) Ref. 35. g) Solid at 25 °C. h) Ref. 56. i) Ref. 57. j) Ref. 58. k) Ref. 12. l) Ref. 59. m) Estimated from Figure 3. n) Ref. 60. o) Ref. 47.

phobic cations are shown in Table 3. When $C_nF_{2n+1}BF_3^-$ are combined with C_8mim^+, T_m increases with increasing n, whereas when combined with TBA^+ and THA^+, T_m decreases with increasing n, except for $[THA^+][C_2F_5BF_3^-]$ that shows low T_m, 19 °C. Other physicochemical properties are listed in Table 3 for the ILs that are in liquid form at room temperature. ILs of longer-chain $C_nF_{2n+1}BF_3^-$ show lower density as seen in $[C_8mim^+][C_nF_{2n+1}BF_3^-]$ ($n = 2$, 3, and 4) and $[THA^+][C_nF_{2n+1}BF_3^-]$ ($n = 2$ and 6). The tendency is similar to that of the $C_nF_{2n+1}BF_3^-$-based ILs with less hydrophobic cations.[24,30,32] The viscosity and the conductivity of $[C_8mim^+][C_nF_{2n+1}BF_3^-]$ in the present study are comparable to those of $[C_mmim^+][C_nF_{2n+1}BF_3^-]$ with smaller m previously reported.[24] However, the viscosity and the conductivity of $[TBA^+][C_6F_{13}BF_3^-]$, $[THA^+][C_2F_5BF_3^-]$, and $[THA^+][C_6F_{13}BF_3^-]$ is much higher and lower, respectively, than those of ILs composed of $C_nF_{2n+1}BF_3^-$ and short-chain quaternary ammonium ions,[30] due to the larger size and the smaller mobility of TBA^+ and THA^+. With increasing n of $C_nF_{2n+1}BF_3^-$ in ILs, the viscosity increases and the conductivity decreases. This tendency was also confirmed for $C_nF_{2n+1}BF_3^-$-based ILs of moderately hydrophobic cations.[24,30,32]

Solubility of ILs of $C_nF_{2n+1}BF_3^-$ in Water. The solubility of $[C_8mim^+][C_nF_{2n+1}BF_3^-]$ in W is listed in Table 3. The values are 5.3, 1.8, and 0.95 mM for $n = 2$, 3, and 4, respectively, and become smaller with increasing n. These values are comparable to 1.6 mM, that of $[C_8mim^+][C_1C_1N^-]$,[12] which is in harmony with the comparable hydrophobicity of $C_nF_{2n+1}BF_3^-$ ($n = 2$, 3, and 4) to $C_1C_1N^-$ (Table 2). For $[TBA^+][C_6F_{13}BF_3^-]$, $[THA^+][C_2F_5BF_3^-]$, and $[THA^+][C_6F_{13}BF_3^-]$, the solubility was not measured because ions constituting the ILs do not show measurable absorption of UV and visible light.

A thermodynamic relationship correlates the solubility of ILs in W with the standard ion-transfer potentials of ions, as shown below,[45]

$$\Delta(\Delta_R^W\phi^0)_{CA} \equiv \Delta_R^W\phi^0_{A-} - \Delta_R^W\phi^0_{C+} = -\frac{RT}{F}\ln K_s^W \quad (2)$$

where K_s^W is the solubility product of ILs in W, $\Delta_R^W\phi_i^0$ is the standard ion-transfer potentials of ions i (i: C^+, A^-) across the IL|W interface, and $\Delta(\Delta_R^W\phi^0)_{CA}$ is the difference of the $\Delta_R^W\phi_i^0$. K_s^W is the square of the solubility of ILs in W, $S_{R/W}^2$, when assuming that the activity coefficients of ions are unity and that the contribution of other ions is negligible. We have found for several cases that there is a linear relationship between $\Delta_R^W\phi_i^0$ and $\Delta_{NB}^W\phi^0_{i,app}$,[46,47] that is,

$$\Delta_R^W\phi_i^0 = a\Delta_{NB}^W\phi^0_{i,app} + b \quad (3)$$

where b is the intercept at $\Delta_{NB}^W\phi_i^0 = 0$, and a is a scaling constant indicating how hydrophobic the IL is as a solvent compared with NB; a values less than unity mean that the IL is more hydrophobic than NB, and vice versa. From eqs 2 and 3

$$\log S_{R/W} = -\frac{2F}{2.303RT}\{a(\Delta(\Delta_{NB}^W\phi^0)_{CA,app})\} \quad (4)$$

where $\Delta(\Delta_{NB}^W\phi^0)_{CA,app}$ is $\Delta_{NB}^W\phi^0_{A^-,app} - \Delta_{NB}^W\phi^0_{C^+,app}$. The relationship between $S_{R/W}$ and $\Delta(\Delta_{NB}^W\phi^0)_{CA,app}$ is shown in Figure 3 for the ILs listed in Table 3. There is good linearity between $\log S_{R/W}$ and $\Delta(\Delta_{NB}^W\phi^0)_{CA,app}$ in a wide range of $S_{R/W}$

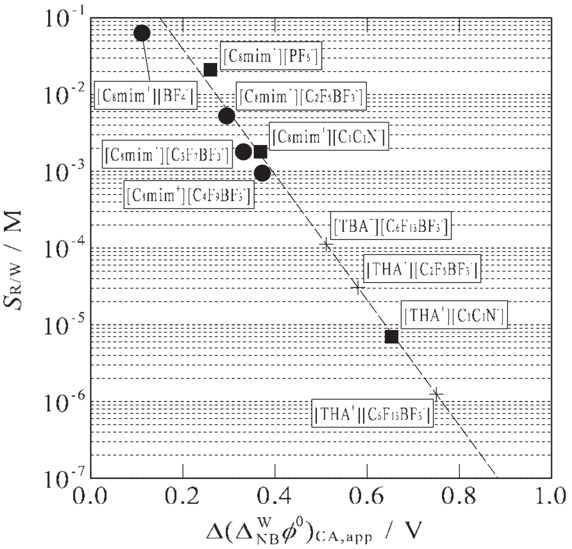

Figure 3. Dependence of the solubility of ILs in water on the difference in the apparent standard ion-transfer potentials of the IL-constituent cations and anions across the NB|W interface for $C_nF_{2n+1}BF_3^-$-based ILs (solid circle), and other ILs (solid square). The broken line is a linear regression line from the plots except for $[C_8mim^+][BF_4^-]$ (**1**), which is used to estimate the solubility of ILs (cross).

from 100 to 0.01 mM, not only for $C_nF_{2n+1}BF_3^-$-based ILs (solid circle) but also for other ILs (solid square). The plot of $[C_8mim^+][BF_4^-]$ (solid circle, **1**) deviated from the straight line to lower solubility, probably due to lower a compared with the other ILs or difficulty of measuring $S_{R/W}$ hampered by non-negligible hydrolysis during the IL–W two-phase equilibrium. The linear regression line from the plots except for $[C_8mim^+][BF_4^-]$ leads to the intercept, -0.03 ± 0.03, and the a value, 0.97 ± 0.09. This result indicates that these ILs have hydrophobicity similar to that of NB, as was previously shown for $[THA^+][C_1C_1N^-]$[45] and trioctylmethylammonium bis(nonafluorobutylsulfonyl)imide.[9] This result is also in harmony with our suggestion that $\Delta_{NB}^{W}\phi_{i,app}^{0}$ is a good measure of $\Delta_{R}^{W}\phi_{i}^{0}$. The straight line enables us to estimate the $S_{R/W}$ values of ILs: 0.1, 0.04, and 0.002 mM for $[TBA^+][C_6F_{13}BF_3^-]$, $[THA^+][C_2F_5BF_3^-]$, and $[THA^+][C_6F_{13}BF_3^-]$, respectively. These µM-level solubilities imply that the interface between W and these ILs is polarizable, as is the case of other highly hydrophobic ILs having µM-level solubility in W.[40,47,48]

Polarized Potential Window. When ILs are composed of highly hydrophobic cations and anions, the IL|W interface is polarizable.[40,45,49–52] If the ions for the electrolyte in W are hydrophilic enough, the width of the polarized potential window (ppw) is determined by the hydrophobicity of the ions constituting ILs and is a good measure of $\Delta(\Delta_{R}^{W}\phi^0)_{CA}$.[45,47] CVs measured to evaluate the width of the ppw of the IL|W interfaces are shown in Figure 4. The CVs showed the ppw depending on the hydrophobicity of the ions constituting the ILs. For $[C_8mim^+][C_2F_5BF_3^-]$ (**1**) and $[C_8mim^+][C_3F_7BF_3^-]$ (**2**) the hydrophobicity of the ILs is not enough to make the IL|W interfaces polarized. For more hydrophobic ILs, $[C_8mim^+][C_4F_9BF_3^-]$ (**3**), $[THA^+][C_2F_5BF_3^-]$ (**4**), $[THA^+][C_6F_{13}BF_3^-]$ (**5**), and $[TBA^+][C_6F_{13}BF_3^-]$ (**6**), the IL|W interfaces are polarized with different widths of the ppw depending on the hydrophobicity of the ILs. It should be noted that the potentials of the negative end of the ppw is almost the same for all the ILs. This is because at the negative end the phase-boundary potential is close to $\Delta_{R}^{W}\phi_{C+}^{0}$ of the cations constituting ILs, but it is canceled out with the phase-boundary potential across the $IL|W_{ref}$ interface determined by the partition of the cations (Scheme 1). The width of the ppw is relativistic but here we evaluated the ppw by defining it as the potential range within which the absolute magnitude of current density does not exceed 0.50 mA cm^{-2}. The current density corresponds to 1.0 nA for the data with the inner diameter of the micropipette tip of 16 µm (data except **6**) and to 0.76 nA for that of 15 µm. The dependence of the ppw on the $\Delta(\Delta_{NB}^{W}\phi^0)_{CA,app}$ is shown in Figure 5. Similar to the solubility (Figure 3), the width of the ppw showed a linearity with $\Delta(\Delta_{NB}^{W}\phi^0)_{CA,app}$. The slope of the linear regression line, 0.92 ± 0.05, is almost the same as the a value evaluated from the solubility, 0.97 ± 0.09. The horizontal intercept of the line is $+0.29 \pm 0.03$ V. This $\Delta(\Delta_{NB}^{W}\phi^0)_{CA,app}$ value is minimum for the IL|W interface to be polarized at this current scale.

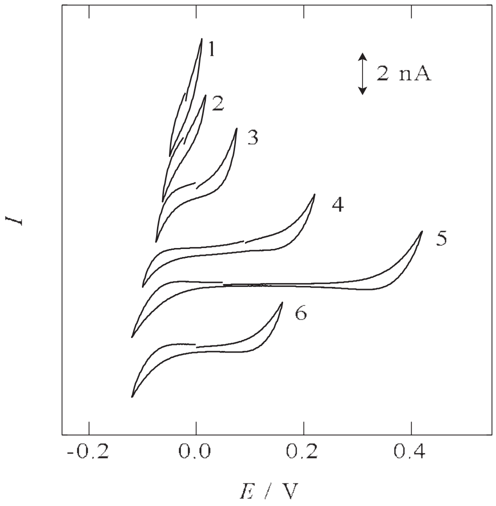

Figure 4. Cyclic voltammograms at the interfaces between water and $[C_8mim^+][C_2F_5BF_3^-]$ (**1**), $[C_8mim^+][C_3F_7BF_3^-]$ (**2**), $[C_8mim^+][C_4F_9BF_3^-]$ (**3**), $[THA^+][C_2F_5BF_3^-]$ (**4**), $[THA^+][C_6F_{13}BF_3^-]$ (**5**), and $[TBA^+][C_6F_{13}BF_3^-]$ (**6**). Scan rate: 10 mV s^{-1}. Inner diameter of the micropipette: 16 µm except **6** (15 µm).

Conclusion

A series of $C_nF_{2n+1}BF_3^-$ ($n = 2$–4 and 6) is found to be suitable for hydrophobic ILs for IL–W two-phase systems. A good correlation is found for the solubility of the ILs in W, the width of the ppw at the IL|W interface, and the apparent standard ion-transfer potentials across the NB|W interface for $C_nF_{2n+1}BF_3^-$ ions. The correlation can be used to estimate an unknown value from the other two. One can tune the polarizability of the IL|W interface from nonpolarized to widely polarizable. The former is indispensable for the application of hydrophobic ILs to salt bridges[10–12] and the latter to ion selective electrodes.[9]

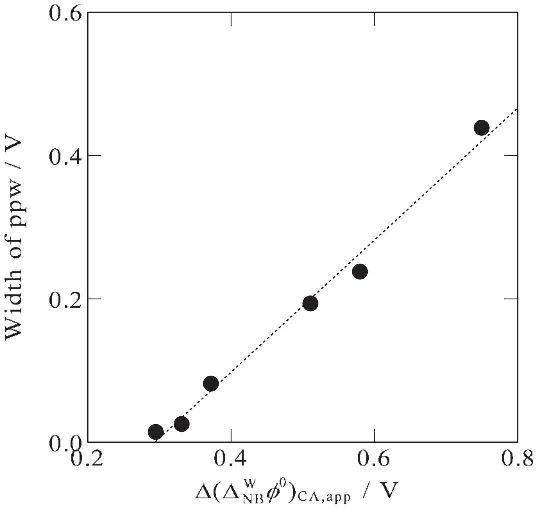

Figure 5. Dependence of the width of the polarized potential window on the difference in the apparent standard ion-transfer potentials of the IL-constituent cations and anions across the NB|W interface for $C_nF_{2n+1}BF_3^-$-based ILs. The dotted line is a linear regression line.

The authors are grateful to Mr. Satoshi Akasaka (Department of Polymer Chemistry, Graduate School of Engineering, Kyoto University) for the DSC measurements. This work was supported by Japan Science and Technology Agency under the program, “Development of Systems and Technology for Advanced Measurement and Analysis.” This work was also partially supported by a Grant-in-Aid for Exploratory Research (No. 17655031) and a Grant-in-Aid for Priority Area (No. 20031017), and by the Global COE Program “International Center for Integrated Research and Advanced Education in Materials Science” (No. B-09) from the Ministry of Education, Culture, Sports, Science and Technology, Japan.

References

1 J. G. Huddleston, H. D. Willauer, R. P. Swatloski, A. E. Visser, R. D. Rogers, *Chem. Commun.* **1998**, 1765.

2 S. Dai, Y. H. Ju, C. E. Barnes, *J. Chem. Soc., Dalton Trans.* **1999**, 1201.

3 A. E. Visser, R. P. Swatloski, W. M. Reichert, S. T. Griffin, R. D. Rogers, *Ind. Eng. Chem. Res.* **2000**, *39*, 3596.

4 S. G. Cull, J. D. Holbrey, V. Vargas-Mora, K. R. Seddon, G. J. Lye, *Biotechnol. Bioeng.* **2000**, *69*, 227.

5 M. Eckstein, M. V. Filho, A. Liese, U. Kragl, *Chem. Commun.* **2004**, 1084.

6 H. Pfruender, M. Amidjojo, U. Kragl, D. Weuster-Botz, *Angew. Chem., Int. Ed.* **2004**, *43*, 4529.

7 C. Coll, R. H. Labrador, R. M. Mañez, J. Soto, F. Sancenón, M.-J. Seguí, E. Sanchez, *Chem. Commun.* **2005**, 3033.

8 N. V. Shvedene, D. V. Chernyshov, M. G. Khrenova, A. A. Formanovsky, V. E. Baulin, I. V. Pletnev, *Electroanalysis* **2006**, *18*, 1416.

9 N. Nishi, H. Murakami, Y. Yasui, T. Kakiuchi, *Anal. Sci.* **2008**, *24*, 1315.

10 T. Kakiuchi, T. Yoshimatsu, *Bull. Chem. Soc. Jpn.* **2006**, *79*, 1017.

11 T. Yoshimatsu, T. Kakiuchi, *Anal. Sci.* **2007**, *23*, 1049.

12 T. Kakiuchi, T. Yoshimatsu, N. Nishi, *Anal. Chem.* **2007**, *79*, 7187.

13 C. A. Wamser, *J. Am. Chem. Soc.* **1948**, *70*, 1209.

14 M. Anbar, S. Guttmann, *J. Phys. Chem.* **1960**, *64*, 1896.

15 C. Villagrán, M. Deetlefs, W. R. Pitner, C. Hardacre, *Anal. Chem.* **2004**, *76*, 2118.

16 H. S. Gutowsky, D. W. McCall, C. P. Slichter, *J. Chem. Phys.* **1953**, *21*, 279.

17 I. G. Ryss, V. B. Tul’chinskii, *Russ. J. Inorg. Chem.* **1964**, *9*, 461.

18 A. E. Gebala, M. M. Jones, *J. Inorg. Nucl. Chem.* **1969**, *31*, 771.

19 M. J. Earle, U. Hakala, B. J. McAuley, M. Nieuwenhuyzen, A. Ramani, K. R. Seddon, *Chem. Commun.* **2004**, 1368.

20 D. B. Williams, M. E. Stoll, B. L. Scott, D. A. Costa, W. J. Oldham, Jr., *Chem. Commun.* **2005**, 1438.

21 M. Castriota, T. Caruso, R. G. Agostino, E. Cazzanelli, W. A. Henderson, S. Passerini, *J. Phys. Chem. A* **2005**, *109*, 92.

22 Y. Yasui, N. Nishi, Y. Kitazumi, T. Kakiuchi, in preparation.

23 R. D. Chambers, H. C. Clark, C. J. Willis, *J. Am. Chem. Soc.* **1960**, *82*, 5298.

24 Z.-B. Zhou, H. Matsumoto, K. Tatsumi, *Chem.—Eur. J.* **2004**, *10*, 6581.

25 H.-J. Frohn, V. V. Bardin, *Z. Anorg. Allg. Chem.* **2001**, *627*, 15.

26 Z.-B. Zhou, M. Takeda, M. Ue, *J. Fluorine Chem.* **2004**, *125*, 471.

27 Z.-B. Zhou, H. Matsumoto, K. Tatsumi, *Chem. Lett.* **2004**, *33*, 680.

28 Z.-B. Zhou, H. Matsumoto, K. Tatsumi, *Chem. Lett.* **2004**, *33*, 886.

29 Z.-B. Zhou, H. Matsumoto, K. Tatsumi, *Chem. Lett.* **2004**, *33*, 1636.

30 Z.-B. Zhou, H. Matsumoto, K. Tatsumi, *Chem.—Eur. J.* **2005**, *11*, 752.

31 H. Matsumoto, Z.-B. Zhou, H. Sakaebe, K. Tatsumi, *Electrochemistry* **2005**, *73*, 633.

32 Z.-B. Zhou, H. Matsumoto, K. Tatsumi, *Chem.—Eur. J.* **2006**, *12*, 2196.

33 Z.-B. Zhou, M. Takeda, M. Ue, *J. Fluorine Chem.* **2003**, *123*, 127.

34 T. Kakiuchi, N. Tsujioka, S. Kurita, Y. Iwami, *Electrochem. Commun.* **2003**, *5*, 159.

35 J. L. Anthony, E. J. Maginn, J. F. Brennecke, *J. Phys. Chem. B* **2001**, *105*, 10942.

36 T. Kasahara, N. Nishi, M. Yamamoto, T. Kakiuchi, *Langmuir* **2004**, *20*, 875.

37 A. J. Bard, L. R. Faulkner, in *Electrochemical Methods*, 2nd ed., John Wiley, New York, **2001**, Chap. 6.

38 T. Ohkouchi, T. Kakutani, M. Senda, *Bioelectrochem. Bioenerg.* **1991**, *25*, 71.

39 N. Tsujioka, S. Imakura, N. Nishi, T. Kakiuchi, *Anal. Sci.* **2006**, *22*, 667.

40 N. Nishi, S. Imakura, T. Kakiuchi, *Anal. Chem.* **2006**, *78*, 2726.

41 K. Kuhlmann, D. M. Grant, *J. Phys. Chem.* **1964**, *68*, 3208.

42 M. J. Frisch, G. W. Trucks, H. B. Schlegel, G. E. Scuseria, M. A. Robb, J. R. Cheeseman, J. A. Montgomery, Jr., T. Vreven, K. N. Kudin, J. C. Burant, J. M. Millam, S. S. Iyengar, J. Tomasi, V. Barone, B. Mennucci, M. Cossi, G. Scalmani, N. Rega, G. A. Petersson, H. Nakatsuji, M. Hada, M. Ehara, K. Toyota, R.

Fukuda, J. Hasegawa, M. Ishida, T. Nakajima, Y. Honda, O. Kitao, H. Nakai, M. Klene, X. Li, J. E. Knox, H. P. Hratchian, J. B. Cross, C. Adamo, J. Jaramillo, R. Gomperts, R. E. Stratmann, O. Yazyev, A. J. Austin, R. Cammi, C. Pomelli, J. W. Ochterski, P. Y. Ayala, K. Morokuma, G. A. Voth, P. Salvador, J. J. Dannenberg, V. G. Zakrzewski, S. Dapprich, A. D. Daniels, M. C. Strain, O. Farkas, D. K. Malick, A. D. Rabuck, K. Raghavachari, J. B. Foresman, J. V. Ortiz, Q. Cui, A. G. Baboul, S. Clifford, J. Cioslowski, B. B. Stefanov, G. Liu, A. Liashenko, P. Piskorz, I. Komaromi, R. L. Martin, D. J. Fox, T. Keith, M. A. Al-Laham, C. Y. Peng, A. Nanayakkara, M. Challacombe, P. M. W. Gill, B. Johnson, W. Chen, M. W. Wong, C. Gonzalez, J. A. Pople, *Gaussian 03, revision B.01*, Gaussian, Inc., Pittsburgh PA, **2003**.

43 R. E. Mesmer, A. C. Rutenberg, *Inorg. Chem.* **1973**, *12*, 699.

44 S. Tanaka, Y. Matsuoka, Y. Kitazumi, N. Nishi, T. Kakiuchi, in preparation.

45 T. Kakiuchi, N. Tsujioka, *Electrochem. Commun.* **2003**, *5*, 253.

46 T. Kakiuchi, N. Tsujioka, K. Sueishi, N. Nishi, M. Yamamoto, *Electrochemistry* **2004**, *72*, 833.

47 N. Nishi, T. Kawakami, F. Shigematsu, M. Yamamoto, T. Kakiuchi, *Green Chem.* **2006**, *8*, 349.

48 N. Nishi, R. Ishimatsu, M. Yamamoto, T. Kakiuchi, *J. Phys. Chem. C* **2007**, *111*, 12461.

49 B. M. Quinn, Z. Ding, R. Moulton, A. J. Bard, *Langmuir* **2002**, *18*, 1734.

50 H. Katano, H. Tatsumi, *Anal. Sci.* **2003**, *19*, 651.

51 R. Ishimatsu, N. Nishi, T. Kakiuchi, *Chem. Lett.* **2007**, *36*, 1166.

52 J. Langmaier, Z. Samec, *Electrochem. Commun.* **2007**, *9*, 2633.

53 J. M. Crosthwaite, M. J. Muldoon, J. K. Dixon, J. L. Anderson, J. F. Brennecke, *J. Chem. Thermodyn.* **2005**, *37*, 559.

54 K. R. Harris, M. Kanakubo, L. A. Woolf, *J. Chem. Eng. Data* **2006**, *51*, 1161.

55 M. Kanakubo, K. R. Harris, N. Tsuchihashi, K. Ibuki, M. Ueno, *Fluid Phase Equilib.* **2007**, *261*, 414.

56 J. G. Huddleston, A. E. Visser, W. M. Reichert, H. D. Willauer, G. A. Broker, R. D. Rogers, *Green Chem.* **2001**, *3*, 156.

57 Y. U. Paulechka, A. V. Blokhin, G. J. Kabo, A. A. Strechan, *J. Chem. Thermodyn.* **2007**, *39*, 866.

58 H. Tokuda, S. Tsuzuki, M. A. B. H. Susan, K. Hayamizu, M. Watanabe, *J. Phys. Chem. B* **2006**, *110*, 19593.

59 Sigma-Aldrich web page: http://www.sigmaaldrich.com.

60 H. Matsumoto, H. Kageyama, Y. Miyazaki, *Chem. Lett.* **2001**, 182.